doi: 10.32023/0001-5237/74.2.2

ACTA ASTRONOMICA
Vol. **74** (2024) pp. 113–133

Absolute Parameters of Three F Type Southern Eclipsing Binary Stars: VW Ret, FW Vel, and CW Eri

P. Zasche[1], D. Sürgit[2,3], A. Erdem[2,4], F. Marang and C. A. Engelbrecht[5]

[1] Charles University, Faculty of Mathematics and Physics, Astronomical Institute, V Holešovičkách 2, CZ-180 00, Praha 8, Czech Republic
[2] Astrophysics Research Center and Ulupınar Observatory, Çanakkale Onsekiz Mart University, TR-17100, Çanakkale, Türkiye
[3] Department of Space Sciences and Technologies, Faculty of Science, Çanakkale Onsekiz Mart University, Terzioğlu Kampüsü, TR-17100, Çanakkale, Türkiye
[4] Department of Physics, Faculty of Science, Çanakkale Onsekiz Mart University, Terzioğlu Kampüsü, TR-17100, Çanakkale, Türkiye
[5] Department of Physics, University of Johannesburg, PO Box 524, Auckland Park 2006, South Africa

Received June 12, 2024

ABSTRACT

This study presents the first detailed analysis of three southern eclipsing binaries. Both – light curves and radial velocity curves – were studied together with their period changes, revealing basic physical and orbital properties of these systems. All three stars, VW Ret, FW Vel, and CW Eri are detached binaries with a few days orbital period. Thanks to our detailed analysis we revealed that all the component stars are slightly heavier than the Sun, laying in the mass range between 1.3 $M_\odot$ and 1.6 $M_\odot$. The systems VW Ret, and FW Vel seem to have more dominant secondary components, both in the masses, as well as in luminosities. The system VW Ret is a triple star showing large eclipse times variations with the periodicity of 4 yr. For FW Vel a similar weak variation was also found, but with much lower amplitude of about 56 s only, needed to be independently confirmed. CW Eri shows slightly eccentric orbit ($e = 0.015$), but only very slow apsidal motion. Moreover, its ages for both component do not agree with each other very well. Hence, it provides a challenge for future more detailed modeling of this interesting system.

Key words: *binaries: eclipsing – Stars: fundamental parameters – binaries: spectroscopic.*

1. Introduction

The critical importance of the study of eclipsing binaries for an accurate understanding of stellar structure and evolution has been discussed at length (see,

e.g., Southworth 2012). These systems provide the most precise measures of basic stellar properties in absolute units (Torres *et al.* 2010).

Increases in the volume and precision of observational data allow additional aspects of the physical behavior of these systems to be analyzed (*e.g.*, pulsations, Gaulme and Guzik 2019) and the presence of additional bodies in short orbits (Borkovits *et al.* 2015) and for tests of general relativity and internal structure models to be conducted by tracking the apsidal motion in a system (Claret *et al.* 2021). Accordingly, we have utilized new observational data to analyze three eclipsing binary (EB) systems, which have not been studied in detail before, for a detailed analysis.

2. Selection of Targets

We selected three stars of medium brightness (V ranging between 8 mag and 11 mag), reasonably short orbital periods (2–3 days), lacking any prior detailed analysis, and located in the southern sky to allow observations from the site of the South African Astronomical Observatory (SAAO). As a corollary to increasing the number of EBs subjected to a detailed analysis, our study of these three systems improves the statistics of well-analyzed EBs. At the time of writing, the DEBCat catalog (Southworth 2015) included only twenty-five systems within the above-mentioned ranges of magnitude and period. Moreover, only eight of these systems had primary components with masses in the range covered by the three systems in this study (1.3–1.6 $M_{\odot}$). Our analysis of three further systems inside the above-mentioned ranges adds significantly to the statistics of such systems. Particulars of the studied systems follow:

VW Ret (HD 28456 = GSC 08869-01380 = Gaia DR3 4678279593727349632, $V = 8.73$ mag) was listed in the Michigan catalog of two-dimensional spectral types for HD stars by Houk and Cowley (1975), giving its spectral type as F0V. However, its variability was first discovered by the Hipparcos satellite (Perryman *et al.* 1997), giving its proper orbital period as 2.0847 d. Notwithstanding its relatively high brightness, short period and deep photometric eclipses, there has been no prior analysis of this system.

FW Vel (HD 299334 = GSC 08210-01099 = Gaia DR3 5360432791051782528, $V = 10.54$ mag) was discovered by Strohmeier *et al.* (1964) using Bamberg photographic plates. The orbital period of the system was given as 2.384082 d by Strohmeier (1966), based on observations covering thousands of epochs at that time. Its spectral type was derived as A2 by Spencer Jones and Jackson (1939) and other databases simply adopted this spectral class from the original source. However, this classification is open to question in view of the observed photometric indices (*e.g.*, $B - V = 0.318$ mag) obtained from the Hipparcos satellite ESA (1997), which indicate a later spectral type. Further, the inferred effective temperatures vary from 6764 K (McDonald *et al.* 2017) to 6387 K (Pickles and Depagne

2010). All these results indicate a slightly later spectral type than A2. The only (very brief) photometric study was published by Özer and Sürgit (2017).

CW Eri (HD 19115 = SAO 148743 = Gaia DR3 5152756553745197952, V = 8.44 mag) is the most studied star in our sample. It was discovered as a variable by Strohmeier (1967) using Bamberg photographic plates. However, the derived orbital period in that study was incorrect. A revised value ($P = 2.72837$ d) was published by Chen (1975), who also presented the first analysis of the system's light curve using Russell's model. Subsequently, the photometric light curves of CW Eri were re-analyzed by Mezzetti *et al.* (1980) using Wood's model, and recently also by Overall and Southworth (2024). The only spectroscopic analysis was carried out by Popper (1983). The spectral type was derived by Popper as F1 and F4 for the two components of the system.

This paper presents the first detailed combined photometric and spectroscopic study for these three eclipsing systems.

3. Observational Data

The spectroscopic observations of VW Ret, FW Vel, and CW Eri were conducted using the Spectrograph Upgrade: Newly Improved Cassegrain (SpUpNIC, see Crause *et al.* 2016, 2019 for details) instrument mounted at the Cassegrain focus of the 1.9-m telescope at the South African Astronomical Observatory (SAAO). We used grating four of the spectrograph which has a wavelength coverage of 400–525 nm with a blaze peak at 510 nm and a resolution of 0.062 nm/px (corresponding to a resolution of approximately 80 km/s in RV and an approximate resolving power $R = 3000$ at the wavelength of the Hβ line). We used a slit width of $1\farcs35$ for all spectroscopic observations of these three eclipsing binary systems and the associated RV standards, which were observed contemporaneously. In total, several dozens of spectra were obtained for the systems during the seasons 2017–2018. All of them are listed below.

The arc spectra were taken as comparison spectra using a Cu/Ar lamp before and after each stellar image in all observations. A set of Quartz-Iodine lamp images was also taken every night for flat-field calibrations. The tasks in the IRAF package were used for the spectral data reduction and calibrations. An example of the observed spectra for each of our stars – VW Ret, FW Vel, and CW Eri – is shown in Fig. 1. The characteristic lines of middle F-type stars are seen in the spectra of all the targets.

3.1. Radial Velocities

The cross-correlation technique (CCT) in the RV package of IRAF (Tonry and Davis 1979, Popper and Jeong 1994) was used to derive RVs of the components of VW Ret, FW Vel, and CW Eri. The MgII (4481) line, which is the most prominent line, was used for RV measurements of VW Ret, FW Vel, and CW Eri. The metallic

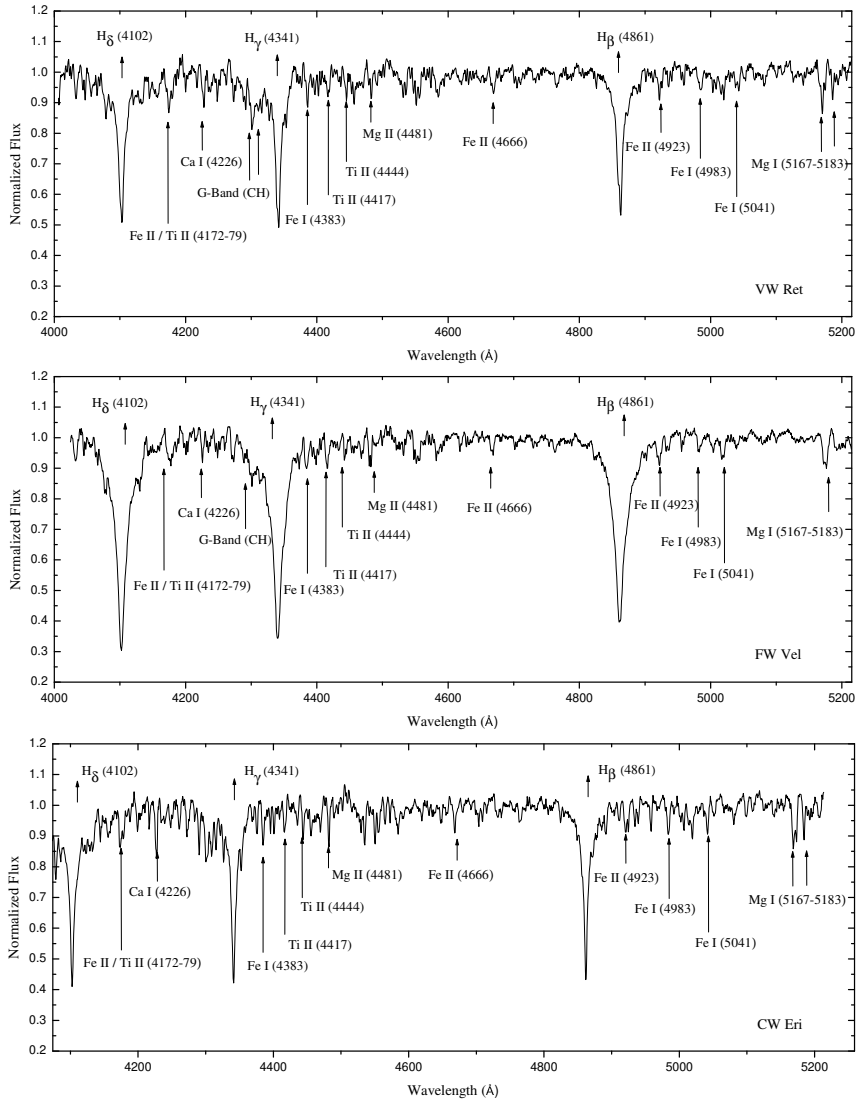

Fig. 1. Sample spectrum of VW Ret, FW Vel, and CW Eri observed at the orbital phase ~ 0.5. Hydrogen Balmer lines and several metallic lines are marked in the spectra.

lines (TiII 4468, MgII 4481, FeII/TiII 4550, and FeII 4584) in the spectral region 4450–4600 Å (see Fig. 1) were used for the cross-correlation measurements of the systems.

The spectra of HD 693, HR 3383, and HR 6031 were used as templates for determining the RVs of the components of VW Ret, FW Vel, and CW Eri. The measured RVs of the components, determined using the cross-correlation method, are listed in Tables 1–3 for VW Ret, FW Vel, and CW Eri, respectively. The EL-EMDR77 program developed by T. Pribulla* was used to determine the orbital pa-

https://www.astro.sk/∼pribulla/soft.html

rameters of VW Ret and FW Vel. During the iterations, circular orbits were assumed for VW Ret and FW Vel. We kept the orbital periods (P) constant at the values obtained through the $O-C$ analysis performed in this study (see Table 4). The RV semi-amplitudes (K_1 and K_2) of the components, the systemic velocity (gamma), and the epoch of minimum RV (T_0) were taken as the free/adjusted parameters for each system.

T a b l e 1

RV measurements of the star VW Ret

Time [HJD-2450000]	RV_1 [km/s]	σ_1 [km/s]	RV_2 [km/s]	σ_2 [km/s]	Time [HJD-2450000]	RV_1 [km/s]	σ_1 [km/s]	RV_2 [km/s]	σ_2 [km/s]
58438.3495			96.95	7.95	58391.4893	106.82	28.41	−88.19	8.90
58438.3576	−68.52	28.31	104.49	7.00	58439.4402	105.65	19.82	−70.82	9.46
58438.3658	−73.54	27.82	109.95	6.43	58391.4946	105.02	28.99	−89.99	8.72
58390.4792	−89.75	22.51	105.37	8.23	58391.5001			−90.51	8.31
58390.4852	−97.95	21.34	107.61	8.11	58437.3643			−86.83	6.49
58390.4907	−103.86	21.36	108.66	8.44	58439.4514	109.59	20.59		
58390.4963	−85.88	22.16	112.61	7.96	58391.5057			−92.42	7.40
58390.5015	−87.65	21.18	117.80	10.89	58437.3702	110.14	23.20	−73.28	8.46
58390.5064	−98.22	21.47	117.67	9.91	58437.3786	120.65	21.55		
58388.4885	−106.33	23.87	109.73	8.17	58439.4733	123.06	23.22		
58388.4934	−108.88	23.25	114.14	8.47	58391.5522	119.13	53.53	−107.31	6.87
58388.4982	−107.49	22.98	112.05	7.93	58389.4723	111.60	37.77	−93.86	7.62
58388.5030	−104.39	23.00	115.15	7.90	58391.5570	118.76	48.69	−104.21	6.95
58388.5076	−111.24	22.82	118.74	10.44	58391.5615			−106.22	6.51
58432.3585	−98.80	17.28	115.89	6.34	58389.4772			−104.06	7.00
58432.3643	−106.46	16.02	122.06	6.79	58389.4820	119.60	22.20	−96.30	8.10
58386.5065			107.67	7.52	58389.4869			−98.29	7.46
58432.3707			119.35	6.90	58389.4926			−96.67	7.27
58432.3768	−103.75	21.53	128.23	6.08	58389.4986			−97.76	7.02
58386.5152			114.00	6.94	58437.5525	121.80	29.31	−96.26	7.68
58432.3828	−94.64	19.73	126.97	6.31	58437.5609			−101.38	7.04
58386.5285			113.58	7.77	58431.3488	138.78	35.29		
58432.4256			133.77	6.76	58431.3548	126.32	26.20		
58430.3693	−98.13	19.71	123.55	6.76	58431.3605	130.53	30.49		
58430.3758	−97.64	14.49	124.04	7.00	58431.3665	140.43	36.82		
58430.3813	−98.67	20.87	126.48	6.68	58431.4160	128.21	24.96		
58430.3860	−93.69	18.21	128.00	6.46	58431.4218	126.19	25.43		
58430.3912			126.68	6.60	58431.4285	135.02	40.08		
58384.5435			100.06	7.99	58431.4352	130.12	31.69		
58384.5497	−96.17	21.81	105.97	7.24	58431.4410	128.49	27.75		
58384.5543	−104.21	18.37	101.41	6.42	58383.5356	124.79	24.75	−84.22	8.30
58430.5097	−66.24	25.32	96.51	7.42	58383.5403	114.58	20.02	−83.98	8.96
58430.5154	−72.12	24.35	94.08	8.22	58383.5450	105.69	21.58	−85.89	8.42
58430.5213			98.29	7.34	58383.5495			−82.81	7.70
58430.5271			99.05	6.80	58383.5540	114.71	21.93	−76.99	5.72
58430.5328			94.91	7.59	58383.5838	116.27	26.81	−75.33	7.51
58391.4842	105.03	27.87	-86.50	9.51	58383.5883			−71.86	7.33

The RV measurements and orbital parameters of the components of CW Eri were derived for the first time by Popper (1983). In this study, the orbit was at first solved assuming it to be circular ($e = 0$). When the TESS light curve of the

T a b l e 2

RV measurements of the star FW Vel

Time [HJD-2450000]	RV_1 [km/s]	σ_1 [km/s]	RV_2 [km/s]	σ_2 [km/s]
57766.4473	−102.71	12.36	79.54	22.33
57766.4592	−92.62	12.51	93.48	19.22
57766.4710	−89.21	14.11	102.87	17.66
57771.4257	−128.28	16.56	102.07	28.33
57771.4366	−127.14	20.68	108.07	18.22
57771.4471	−129.38	13.91	108.59	25.66
57771.4601	−118.52	10.57	123.01	29.22
57771.5492	−121.58	16.25	88.90	26.20
57771.5577	−115.69	14.88	97.38	23.40
57771.5661	−123.29	8.48		
57767.5258	39.02	33.20	−57.08	12.11
57772.4290	81.20	25.30	−96.31	11.27
57772.4389	80.23	18.07	−98.03	9.41
57772.4499			−110.08	7.28
57772.5568	102.49	15.85	−105.20	7.89
57772.5660	113.41	14.44	−112.46	7.29
57765.4473	125.74	11.41	−105.12	9.22
57765.4555	121.51	18.53	−99.26	8.55
57765.4636	121.55	18.05	−96.06	8.96
57765.5732	113.83	17.44	−83.73	24.30
57765.5835	113.23	15.66	−79.53	23.22
57770.4660	71.06	27.55	−90.25	25.22
57770.4890	56.07	33.20	−81.47	12.23
57770.5004	66.15	25.33	−81.97	11.22

system was analyzed for the photometric solution, it revealed a very small value of eccentricity, which we adopted in the following analysis. In the orbital solution for CW Eri, the eccentricity (e) and the argument of periastron (ω) were both obtained from the photometric solution. The orbital period was also derived from the $O-C$ analysis. The RV semi-amplitudes (K_1 and K_2) of the components, the systemic velocity (γ), and the epoch of minimum RV (T_0) were taken as the free/adjusted parameters. Finally, we determined the orbital parameters of VW Ret, FW Vel, and CW Eri, as listed in Table 4. These parameter values served as the initial values for our combined fitting of light curves and RV curves, as elucidated in Section 4.

3.2. Photometry

Two disparate sources of photometric data were used. First, the very precise data from the TESS satellite (Ricker *et al.* 2015). This superb source of data was used for the modeling of the light curve because of its number of data points, cadence, and precision of individual data points. The following TESS sectors were used for the three systems: sector 61 (data cadence, 158 s) for VW Ret, sector 36

T a b l e 3

RV measurements of the star CW Eri

Time [HJD-2450000]	RV_1 [km/s]	σ_1 [km/s]	RV_2 [km/s]	σ_2 [km/s]	Time [HJD-2450000]	RV_1 [km/s]	σ_1 [km/s]	RV_2 [km/s]	σ_2 [km/s]
58432.3247			148.38	21.47	58384.4778	114.23	5.76	−55.88	34.51
58432.3306			143.85	27.19	58384.4852	115.71	6.49	−53.72	8.33
58432.3372	−47.50	8.11	147.67	22.67	58384.4896	114.89	5.17	−60.12	22.01
58432.3419	−43.76	8.51			58384.5678	123.60	7.11	−73.16	20.44
58432.3466			157.06	21.86	58384.6142	122.95	6.79	−72.18	21.77
58391.4549	−52.85	5.63			58384.6187	126.58	5.77	−73.29	35.34
58391.4599	−45.15	5.28	152.19	22.59	58439.4099	132.09	4.23	−77.23	9.14
58391.4645	−49.10	5.69	153.96	28.84	58439.4203	135.26	4.22	−79.96	10.25
58391.4688	−45.83	5.38	148.22	19.60	58439.4284	135.29	3.94		
58391.4730	−51.01	4.72	148.06	14.43	58431.3162	130.14	5.31	−79.15	6.02
58432.4091	−56.71	5.97	144.53	24.18	58431.3216	132.51	5.46	−78.34	18.17
58432.4147	−59.38	6.09	146.73	19.92	58431.3275	134.33	7.25	−79.45	12.11
58391.5254	−54.67	8.12	154.53	26.69	58431.3329	133.45	6.89	−73.65	18.83
58391.5302	−56.74	5.71	148.86	22.63	58431.3377			−74.91	18.24
58391.5353	−65.19	5.74	159.02	26.17	58390.4329	118.72	5.37	−75.31	15.50
58391.5404	−52.44	6.87	150.89	26.51	58390.4381	125.60	6.41	−74.82	13.67
58391.5455	−55.65	9.47			58390.4433	119.60	5.82	−72.16	15.32
58391.5808	−52.53	9.80	150.01	26.75	58390.4489	126.98	7.27	−74.05	21.88
58391.5863	−57.64	10.55	144.89	29.84	58390.4537	122.58	6.41	−72.09	14.95
58383.4617	−58.22	11.69			58431.3898	121.76	7.80	−71.37	27.57
58383.4697	−49.97	11.21	153.91	22.03	58431.3944	128.49	5.85	−70.91	20.04
58383.4741	−53.44	3.88	151.77	20.12	58431.3987	122.63	6.36	−66.02	24.96
58383.4784	−58.12	4.09	153.71	37.70	58431.4028	120.16	7.40	−63.41	23.55
58383.5683	−56.37	5.81	144.64	22.25	58431.4069	122.14	6.53	−57.98	24.78
58383.5726	−55.49	6.43	146.46	18.42	58390.5216	115.28	15.4	−67.85	20.48
58383.5768	−52.24	5.95	147.17	22.97	58390.5264	117.29	9.52	−62.36	26.89
58389.4475	21.28	5.04			58390.5312	113.37	5.51	−57.01	22.12
58389.4523	24.65	3.58			58390.5362	117.14	5.39	−55.72	31.69
58389.4571	27.39	1.83			58390.5410	114.62	5.58	−53.05	33.59
58389.4613	25.05	1.40			58431.4775	117.69	8.54	−48.83	22.20
58384.4603	118.67	6.88	-57.82	12.36	58431.4813	111.24	9.06	−58.02	24.02
58384.4653	109.26	6.27	-55.63	34.07	58431.4843	107.62	8.81	−54.55	30.27
58384.4709	104.24	6.65	-56.86	13.94	58431.4875	108.40	8.49	−51.84	22.93

(475 s) for FW Vel and sector 31 (475 s) for CW Eri. The photometry was obtained from the TESS archive using the pipeline Lightkurve (Lightkurve Collaboration *et al.* 2018). In total, more than 10 500 data points were used for the sector with 158 s cadence, and 3500 data points for the sectors with 475 s cadence. These data constitute the highest quality photometry available, and the only data of suitable quality for detailed light curve modeling.

The other existing photometric data for the three studied systems were only utilized for analyzing the long-term evolution of the orbits and to detect other effects such as apsidal motion (Giménez and Bastero 1995) and the light-travel-time effect (LTTE) (Mayer 1990). Photometry of a lower quality than the TESS data remains sufficient for these forms of analysis. Typically, the level of photometric precision of these older survey data is approximately an order of magnitude worse than the TESS photometry itself. However, we used our AFP method (Zasche *et*

T a b l e 4

The orbital parameters of VW Ret, FW Vel, and CW Eri obtained from cross-correlation RV measurements

Parameter	VW Ret	FW Vel	CW Eri
P [d]	2.0846323 (fixed)	2.3835168 (fixed)	2.72837080 (fixed)
T_0 [HJD]	59088.4844 ± 0.0044	59282.0128 ± 0.0137	58728.0357 ± 0.0038
e	0	0	0.0146 (fixed)
ω [deg]	–	–	290.49(fixed)
K_1 [km/s]	119.52 ± 1.13	120.28 ± 1.53	96.71 ± 0.55
K_2 [km/s]	113.94 ± 1.06	106.11 ± 1.42	120.73 ± 0.44
V_0 [km/s]	11.49 ± 0.70	-1.94 ± 1.53	37.84 ± 0.46

al. 2014) to derive the individual times of eclipses from the sparse photometric data. The AFP method computes the times of eclipse by shifting the light curve template in the $x-y$ direction on the phased light curves obtained during a considerably shorter time epoch, *e.g.*, one season of data. This method generates a typical uncertainty of approximately 0.001 d for individual times of mid-eclipse, even for poorly-sampled light curves. Sources of these data were: ASAS-3 (2000–2009, Pojmanski 2002) and ASAS-SN (2013–2024, Shappee *et al.* 2014, Kochanek *et al.* 2017) survey data, Hipparcos (1990–1993, Perryman *et al.* 1997), Applause (1963–1976, Groote *et al.* 2014), INTEGRAL/OMC (2003–2022, Mas-Hesse *et al.* 2003), DASCH (1890–1989, Tang *et al.* 2013), and Maehara (2014) (2010–2023, Maehara 2014).

4. The Analysis

The TESS photometry used for VW Ret, FW Vel, and CW Eri was analyzed using the approach of Wilson and Devinney (1971) and its later modifications. Moreover, for better estimation of overall uncertainties of individual parameters we additionally implemented a Monte Carlo (MC) search method as introduced by Zola *et al.* (2004, 2010).

4.1. VW Ret

Several approaches were followed to estimate the effective temperatures of the primary component. First, we determined an effective temperature of 7220 K for the primary component of VW Ret from the calibrated data in Pecaut and Mamajek (2013), in accordance with the system's spectral classification as F0V given by Houk and Cowley (1975). Second, the intrinsic color index $(B-V)_0$ was calculated in accordance with Bilir *et al.* (2008), using B and V magnitudes from the AAVSO Photometric All Sky Survey (APASS) DR9 (Henden *et al.* 2015)

and JHK magnitudes from the 2MASS database (Cutri *et al.* 2003). This method yielded a temperature of 6782 K using the calibrated data in Pecaut and Mamajek (2013). As the third method, the mass values of the components ($M_1 \cong 1.39$ M$_\odot$, $M_2 \cong 1.41$ M$_\odot$) obtained from the RV solution listed in Table 4 imply spectral types close to F5V, corresponding to a temperature of 6550 K for the primary component. This value is in good agreement with the values of effective temperature for VW Ret derived by Bai *et al.* (2019), who quoted 6473 K, and Schofield *et al.* (2019) who quoted 6597 K. The spectral type of the primary component was also estimated as F5V using the line matching method for the Hγ, Hβ, CaI (4226), MgII (4384, 4481, and 4668), FeI (4383), and FeII (4924) lines (see Fig. 1 for VW Ret) in the spectra observed at the conjunction phases of the components compared with sample spectra for F-type main sequence stars in Gray and Corbally (2009). Synthesizing the results from these methods, the temperature of the primary component of VW Ret was fixed at 6550 K in the subsequent WD + MC iterations.

4.2. FW Vel

A similar approach was followed to estimate the effective temperature of the primary component of FW Vel. First, the temperature was determined as 8800 K from the calibrated data in Pecaut and Mamajek (2013), in accordance with the A2 spectral class assigned by Spencer Jones and Jackson (1939). Second, the observational spectroscopic data of FW Vel were compared with the spectral lines for main sequence stars in the F spectral class provided in Gray and Corbally (2009). The spectral class of the primary component was estimated as F5 using the line matching method for Hydrogen Balmer lines (Hβ and Hγ), CaI (4226), MgII (4384, 4481 and 4668), FeI (4383), FeII (4924), and *G*-band (CH) lines. Finally, considering the mass values of the components of FW Vel obtained from the RV solution ($M_1 \cong 1.37$ M$_\odot$, $M_2 \cong 1.52$ M$_\odot$), the calibrations in Pecaut and Mamajek (2013) indicate that the spectral type of FW Vel is close to F5V. Accordingly, the temperature of the primary component was accepted as 6500 K. It is not apparent why the original classification as A2 was so different from the present most probable classification. There is no other similarly bright close star in the vicinity of the target that could account for the misidentification. The only nearby star of similar class appears to be HD 299333, which is approximately 8$'$away. Ofek (2008) also quoted a spectral type of F5.

4.3. CW Eri

We repeated the aforementioned approach for deriving the effective temperature of the primary component of CW Eri. First, the temperature was determined as 6820 K from the calibrations in Pecaut and Mamajek (2013), in accordance with the F2V spectral type quoted by Houk and Smith-Moore (1988). Second, the intrinsic color index $(B-V)_0$ was calculated in accordance with Bilir *et al.* (2008) by using *B, V*, and *JHK* magnitudes. The temperature of the primary component

was thus determined as 7120 K in accordance with Pecaut and Mamajek (2013). Next, considering the mass values of the components of CW Eri from the RV solution ($M_1 \cong 1.61$ M$_\odot$, $M_2 \cong 1.32$ M$_\odot$), the effective temperature of the primary component of CW Eri was estimated as 7220 K from the calibrations in Pecaut and Mamajek (2013). Finally, the observed spectra were compared with spectra for main sequence stars of F type in Gray and Corbally (2009). The spectral class of the primary component of CW Eri was estimated as F3–F4 using the line matching method for Hydrogen Balmer lines (Hβ and Hγ), CaI (4226), MgII (4384, 4481 and 4668), FeI (4383), FeII (4924), and *G*-band (CH) lines. The temperature associated with this spectral type is approximately 6700($\pm$200) K, according to the calibrations in Pecaut and Mamajek (2013). In contrast photometric data imply slightly lower effective temperatures of 6670 K (Gaia Collaboration *et al.* 2023), 6890 K (Wright *et al.* 2003), and (again) 6670 K (Zheng *et al.* 2023), respectively. We fixed the temperature of the primary component at 6700 K for our analysis.

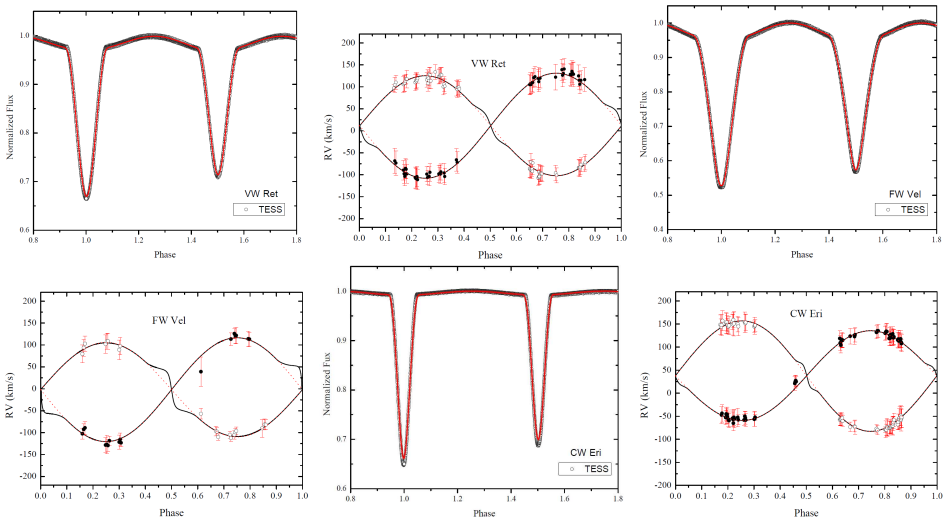

Fig. 2. *Upper plots*: TESS light-curve fits, *Lower plots:* Radial velocity curve fits of VW Ret, FW Vel, and CW Eri.

4.4. Method

The following approach was followed for the entire analysis. After collecting all the available data, we ran the fitting code for both light curves as well as RV curves. From the starting values (taken from the already published papers or from our initial estimate) we converged to the values of some preliminary solution on the radiative and geometrical properties of the stars. Then, such a solution was used for constructing the template light curve for our AFP method for deriving the proper and more reliable value of the period of the whole system.

Only then, after collecting the available photometry covering several decades of data (for example for FW Vel even more than a century now), we were able

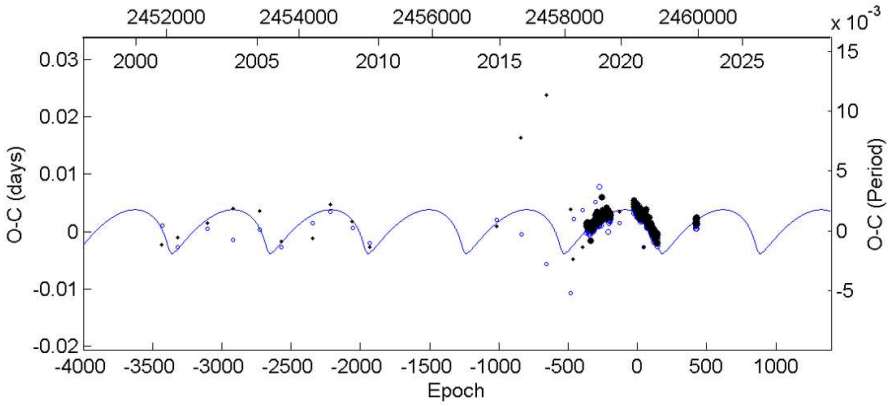

Fig. 3. $O-C$ diagram for the system VW Ret. The final fit is represented by the blue curve. Individual observations are denoted as full dots for the primary eclipses and as open circles for the secondary eclipses. The larger the symbol, the greater the precision.

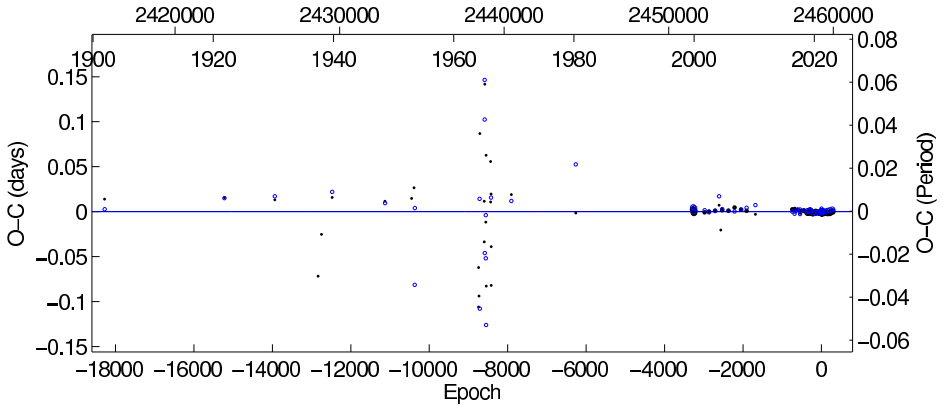

Fig. 4. $O-C$ diagram for the system FW Vel.

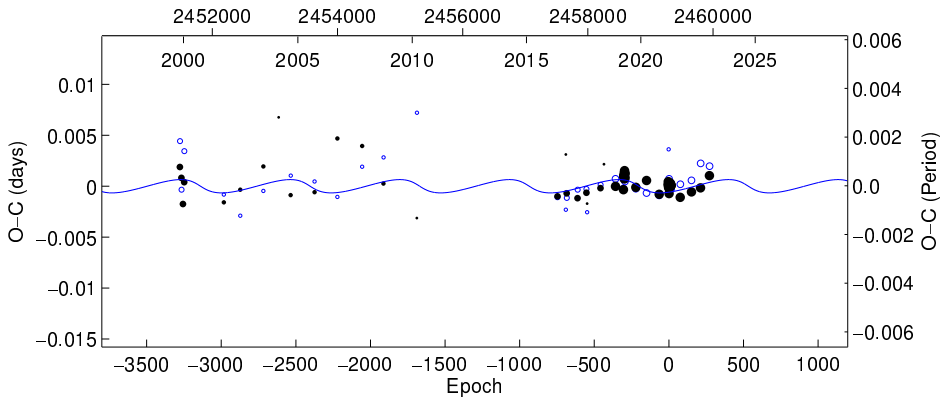

Fig. 5. Diagram of FW Vel after zooming in to the more recent and more precise data. The curve shows the preliminary fit; see the text for details.

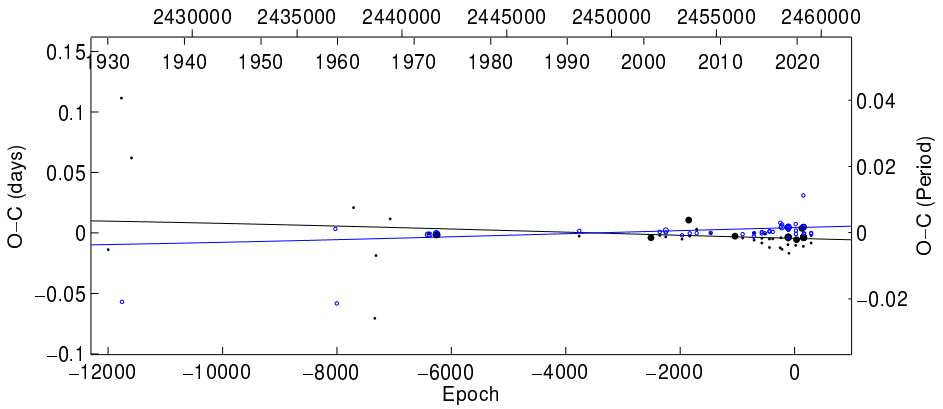

Fig. 6. $O-C$ diagram for the system CW Eri. Primary eclipses are fitted with the black curve; secondary eclipses with the blue curve.

T a b l e 5

Parameters obtained from the LC+RV fitting of VW Ret, FW Vel, and CW Eri

Parameter	VW Ret	FW Vel	CW Eri
T_0 [HJD]	2459088.4800	245281.9831	2458729.2493
P [d]	2.0846323	2.3835168	2.7283708
A [$R_\odot$])	9.71 ± 0.05	10.68 ± 0.10	11.75 ± 0.04
e	–	–	0.0146 ± 0.0006
ω [deg]	–	–	290.49 ± 0.02
$q = M_2/M_1$	1.0488 ± 0.0002	1.1035 ± 0.038	0.815 ± 0.003
i [deg]	82.28 ± 0.14	87.14 ± 0.08	86.19 ± 0.03
T_1 [K]	6550 (fixed)	6500 (fixed)	6700 (fixed)
T_2 [K]	6161 ± 202	6111 ± 204	6495 ± 110
Ω_1	6.271 ± 0.037	5.035 ± 0.006	6.326 ± 0.040
Ω_2	4.834 ± 0.011	4.503 ± 0.004	7.503 ± 0.021
r_1 [mean]	0.193 ± 0.011	0.257 ± 0.011	0.182 ± 0.002
r_2 [mean]	0.275 ± 0.011	0.317 ± 0.014	0.128 ± 0.004
L_1 [TESS]	0.343 ± 0.004	0.430 ± 0.001	0.901 ± 0.020
L_2 [TESS]	0.606 ± 0.004	0.570 ± 0.001	0.099 ± 0.020
L_3 [TESS]	0.051 ± 0.004	–	–

to fix the up-to-date ephemerides of the system to run the reliable analysis. The final resulting values of linear ephemerides were the ones given in our Table 5 derived using all available times of eclipses. The final parameters as derived from the combined analysis of light and RV curves are also given in Table 5. As one can see, a significant fraction of the third light was detected only for the first one system VW Ret. Its level of 5% is normally at the edge of detectability with the standard ground-based data, but which is definitely not the case for the super precise

TESS photometry here. Its resulting value is definitely proved with the nowadays quality of data and one should speculate about origin of such a third component contribution.

On the other hand, the system VW Ret seems to be the one reliably showing also the significant variation in its times of eclipses as were derived from photometry from last decades. Older photometry only barely shows such variation. But now the triple nature of this system seems to be proved. Its small contribution to the total light explains why this third body cannot be detected in the spectra of the system. The orbital parameters of such a third component were derived: period $p_3 = 4.01$ yr, $A = 0.0028$ d, $e_3 = 0.70$. This still rather preliminary solution should be updated with the new observations in the future to confirm or adequately re-calculate this orbit. With the GAIA DR3 (Gaia Collaboration *et al.* 2023) parallax of the system the predicted angular separation of the two components in the sky should be at least 13 mas. We can only speculate whether such an angular distance can be detected with nowadays hi-res technique for a 9-th magnitude star.

A similar behavior was also studied for FW Vel, but only on the more recent precise data spanning a decade back. As one can see in Fig. 5 this putative variation is small enough to be also detected in older data of lower quality. Its fit (period 4.8 yr, amplitude only 56 seconds!) is still only very hypothetical one now and has to be confirmed with future high quality observations.

Another remarkable finding is the fact that the last system in our analysis CW Eri also shows slow apsidal motion. This can only be detected thanks to the precise observations from the last decade, namely using the data from TESS and the ASAS-SN survey (Shappee *et al.* 2014, Kochanek *et al.* 2017). The older photometry is not precise enough for detecting such a small effect (due to its small eccentricity at the level of $e = 0.015$ only).

5. Absolute Parameters

The absolute parameters of VW Ret, FW Vel and CW Eri were calculated by combining the RV solutions and the model parameters from the TESS light curves. Both the systems VW Ret, and FW Vel have the dominant component the secondary instead of primary (if placing the deeper eclipse into the phase 0.0). This is caused by the fact that the secondary components are cooler and inflated more than what one would expect for a main sequence star. All the derived parameters together with their errors are given in Table 6. In the calculations, the effective temperature, bolometric correction, and surface gravity of the Sun were taken as $T_{\rm eff} = 5771.8(\pm 0.7)$ K, $M_{\rm bol} = 4.7554 \pm 0.0004$ mag, $BC = -0.107 \pm 0.02$ mag, and $g = 27423.2 \pm 7.9$ cm/s^2, respectively (Pecaut and Mamajek 2013).

The interstellar absorption and color excess for the systems were computed using the following method. The total absorption toward the system in the Galactic disk in the V band, $A_\infty(V)$, was taken from Schlafly and Finkbeiner (2011), using

the NASA Extragalactic Database[†]. Then, the interstellar absorption corresponding to the distance to the system, $A_d(V)$, was derived from the formula given by Bahcall and Soneira (1980) (in their Eqn. 8), using the system's Gaia-DR3 parallax (Gaia Collaboration *et al.* (2023). Finally, the color excess for the system at the distance d was estimated as $E_d(B-V) = A_d(V)/3.1$.

When considering interstellar reddening for VW Ret, FW Vel and CW Eri in the V-band, the distances to VW Ret, FW Vel and CW Eri were determined as 250 ± 22 pc, 1023 ± 90 pc and 184 ± 15 pc, respectively. According to Popper (1998) photometric parallax formula, the distances to VW Ret, FW Vel and CW Eri, were calculated as 270 ± 15 pc, 1116 ± 30 pc and 190 ± 13 pc, respectively. Based on the parallax value obtained from GAIA DR3 (Gaia Collaboration *et al.* 2023) database, the distances to VW Ret, FW Vel and CW Eri are 270 ± 2 pc, 1143 ± 26 pc and 191 ± 1 pc. The parallax values calculated by three different methods are in good agreement within the error limits.

T a b l e 6

Absolute parameters of VW Ret, FW Vel and CW Eri

	VW Ret		FW Vel		CW Eri	
Parameter	Primary	Secondary	Primary	Secondary	Primary	Secondary
A [$R_\odot$]	9.71 ± 0.05		10.68 ± 0.10		11.75 ± 0.04	
M [$R_\odot$]	1.39 ± 0.02	1.45 ± 0.02	1.37 ± 0.04	1.52 ± 0.04	1.61 ± 0.02	1.32 ± 0.02
R [$R_\odot$]	1.87 ± 0.03	2.67 ± 0.02	2.74 ± 0.14	2.67 ± 0.18	2.14 ± 0.03	1.50 ± 0.05
$logg$ [cm/s^2]	4.034 ± 0.002	3.748 ± 0.001	3.699 ± 0.023	3.559 ± 0.034	3.986 ± 0.051	4.203 ± 0.023
T [K]	6550 ± 200	6161 ± 202	6500 ± 200	6111 ± 220	6700 ± 200	6495 ± 203
L [$L_\odot$]	5.824 ± 0.84	9.256 ± 1.48	12.123 ± 1.14	14.401 ± 2.08	8.31 ± 1.71	3.63 ± 0.641
M_{bol} [mag]	2.83 ± 0.16	2.32 ± 0.17	2.03 ± 0.26	1.84 ± 0.27	2.44 ± 0.17	3.34 ± 0.15
M_V [mag]	2.82 ± 0.16	2.35 ± 0.17	2.02 ± 0.26	1.87 ± 0.27	2.42 ± 0.17	3.33 ± 0.15
$E(B-V$ [mag]	0.014		0.023		0.095	
$B-V$ [mag]	0.22 ± 0.09		0.38 ± 0.07		-0.04 ± 0.14	
V [mag]	8.84 ± 0.02		10.81 ± 0.02^a		8.44 ± 0.02	
M_V system [mag]	1.81 ± 0.18		1.19 ± 0.20		2.03 ± 0.14	
d [pc]	250 ± 22		1023 ± 90		184 ± 15	
d_{Gaia} [pc] DR3	270 ± 2^b		1143 ± 26^b		191 ± 1^b	

Notes: [a] (APASS) DR9,[b] Gaia Collaboration (2023)

6. Evolutionary States

We examined the evolutionary states using the derived physical parameters of VW Ret, FW Vel and CW Eri, according to Geneva stellar evolution models (Ekström *et al.* 2012). Unfortunately, the low resolution of the spectra does not allow us to determine the metallicities of the systems. For the components of each system, (i) The effective temperature *vs.* surface gravity ($\log T - \log g$) diagrams were

[†] *http://ned.ipac.caltech.edu/forms/calculator.html*

used to determine the metallicities of the systems; (ii) The log *age*−*radius* diagrams were then plotted to estimate the ages of the systems, according to these determined metallicities; (iii) The isochrones of estimated ages were checked using the Hertzsprung-Russell (HR) diagrams. The results obtained for each star are shown in Figs. 7–9.

We display the evolutionary tracks interpolated to the measured masses of the components of VW Ret for $Z = 0.01$ taken from Mowlavi *et al.* (2012). The position of the components in $\log T - \log g$ diagram is shown in the upper panel of Fig. 7. Then, we plotted the evolutionary tracks of the masses of the components for $Z = 0.01$ in the log *age*−*radius* diagram in the middle panel of Fig. 7. The measured radius for the primary component corresponds to log $age = 9.40$, while for the secondary component, it is determined as log $age = 9.40$. In this diagram, the masses and radii of both components of VW Ret show perfect agreement with 2.50 Gyr as the age of the system. According to the HR Diagram, it is observed that the primary component is on the terminal-age main-sequence (TAMS), while the secondary component is located beyond the TAMS.

The plots of $\log T - \log g$ diagram for FW Vel using the assumption of $Z = 0.006$ (Eggenberger *et al.* 2021) are presented in the upper panel of Fig. 8. The evolutionary tracks of the masses of the components for $Z = 0.006$ are plotted in the log *age*−*radius* diagram below. The primary radius is in agreement with log $age = 9.44$, while for the secondary component, it is determined as log $age = 9.31$. In this diagram, both the masses as well as radii of FW Vel show good agreement with an age of 2.36 Gyr. Therefore, both the components of FW Vel are evolved and located beyond the TAMS.

We display the positions of both components of CW Eri for $Z = 0.014$ (Mowlavi *et al.* 2012) in the $\log T - \log g$ diagram in the upper panel of Fig. 9. Then, we plotted the evolutionary tracks of the masses of the components for $Z = 0.014$ in the log *age*−*radius* diagram in the middle panel of Fig. 9. The measured radius for the primary component corresponds to log $age = 9.18$, while for the secondary component, it is determined as log $age = 9.37$. The individual isochronal age estimates do not agree well with each other, being most probably in between 1.5 Gyr and 2.5 Gyr. However, it is not clear why such a discrepancy between the two components appears. According to still eccentric orbit and the circularization processes the system should be younger. Another possibility would be to trace the age of the system from its apsidal motion and internal constant. However, its apsidal movement is so small that it could be derived only in TESS precision data. Unfortunately no other future TESS observations of the target are being planned for the future. Just after writing the first version of the manuscript, a new study on CW Eri was posted on arXiv (Overall and Southworth 2024). Their findings are very similar to ours, the individual parameters like masses, radii, or distance are only slightly off the respective error intervals. One can only speculate where such a small discrepancy comes from (at the level of 3%, while the two error bars are

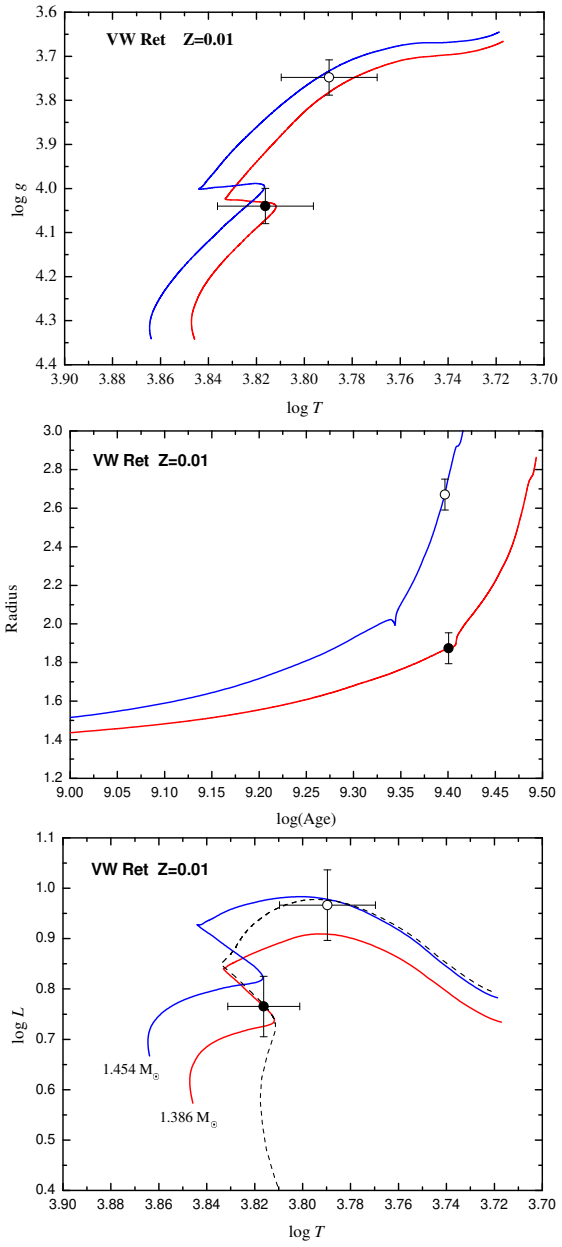

Fig. 7. Geneva Evolution Model of VW Ret: a comparison between the physical parameters and theoretical values of the components: the positions of components of VW Ret in the $\log T - \log g$ diagram for $Z = 0.01$ (Mowlavi *et al.* 2012) are presented in the *upper panel*, the log *age*−*radius* diagram for the measured masses of components in the *middle panel*, and the locations of the components in the HR (Hertzsprung-Russell) diagram in the *lower panel*. The Geneva isochrone line for an age of 2.50 Gyr is indicated by the dashed black curve superimposed on the HR diagram. The colored solid lines for the inscribed masses display the evolutionary tracks of stars with these masses. In all diagrams, filled and open circle symbols represent primary and secondary components, respectively. Vertical and horizontal lines indicate the error bars of the components.

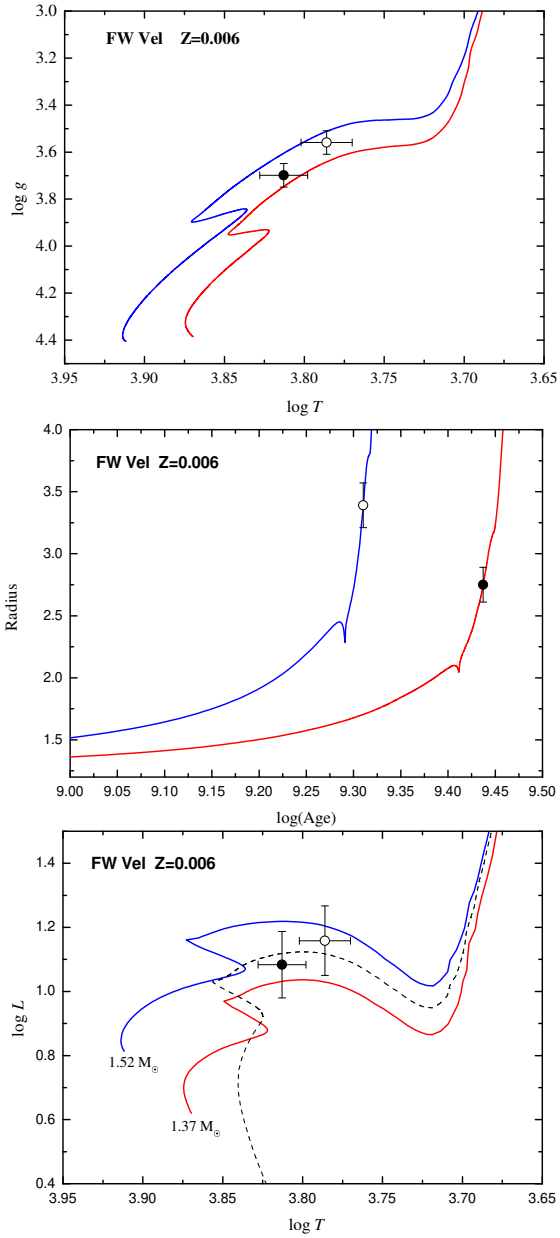

Fig. 8. Geneva Evolution Model of FW Vel: a comparison between the physical parameters and theoretical values of the components: the positions of components of FW Vel in the $\log T - \log g$ diagram for $Z = 0.006$ (Eggenberger *et al.* 2021) are presented in the *upper panel*, the log *age*−*radius* diagram for the measured masses of components in the *middle panel*, and the locations of the components in the HR (Hertzsprung-Russell) diagram in the *lower panel*. The Geneva isochrone line for an age of 2.36 Gyr is indicated by the dashed black curve superimposed on the HR diagram. The colored solid lines for the inscribed masses display the evolutionary tracks of stars with these masses. In all diagrams, filled and open circle symbols represent primary and secondary components, respectively. Vertical and horizontal lines indicate the error bars of the components.

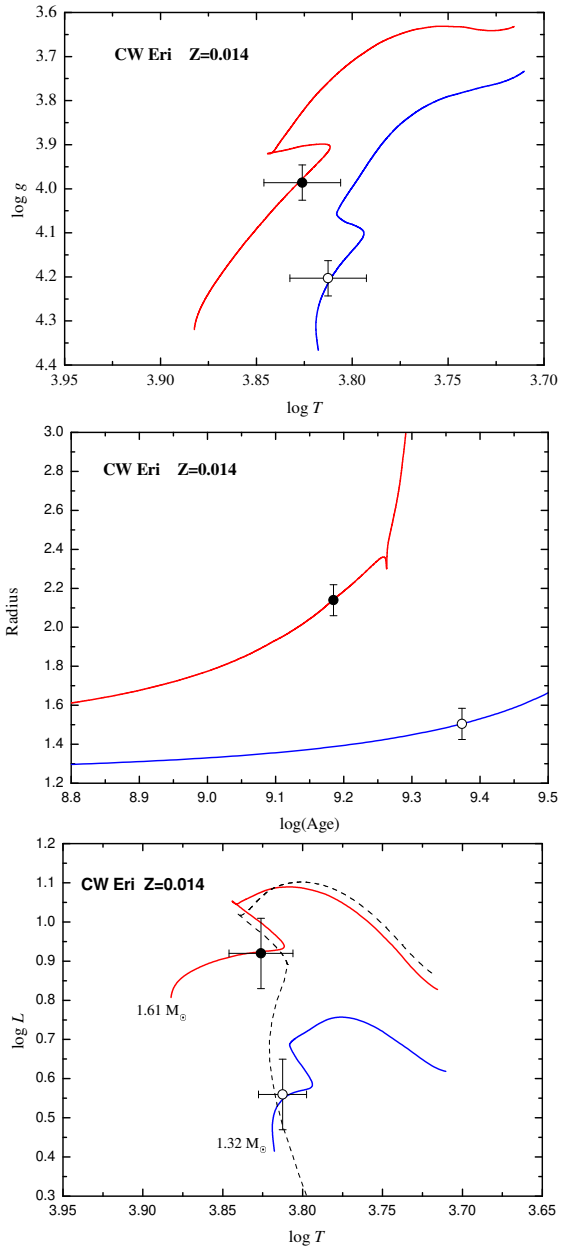

Fig. 9. Geneva Evolution Model of CW Eri: a comparison between the physical parameters and theoretical values of the components: the positions of components of CW Eri in the $\log T - \log g$ diagram for $Z = 0.014$ (Mowlavi *et al.* 2012) are presented in the *upper panel*, the log *age*−*radius* diagram for the measured masses of components in the *middle panel*, and the locations of the components in the HR (Hertzsprung-Russell) diagram in the *lower panel*. The Geneva isochrone line for an age of 1.90 Gyr is indicated by the dashed black curve superimposed on the HR diagram. The colored solid lines for the inscribed masses display the evolutionary tracks of stars with these masses. In all diagrams, filled and open circle symbols represent primary and secondary components, respectively. Vertical and horizontal lines indicate the error bars of the components.

at the level of about 1% for the primary mass, for instance). One possibility is the polynomial fitting for detreding the TESS data used by Overall and Southworth (2024), the other can be the use of other RV data set.

7. Summary

We have studied three rather seldomly-investigated systems VW Ret, FW Vel, and CW Eri and found all of them somehow noteworthy. The first one system VW Ret is in fact a triple star. For planning some future observations this would be an important finding, since its ephemerides are therefore not linear and constant. Proving its nature with more data in the future would also be very useful. For the second system FW Vel such a hypothesis also exists, but is now substantiated on even weaker proofs. Therefore, also here another precise observations would be of high importance.

Another interesting finding was that the system CW Eri shows slightly eccentric orbit and probably slow apsidal motion. However, its modeling is still rather challenging. Its eccentricity is small. Its apsidal motion very slow. And also the individual ages of components as derived from our analysis are not is agreement with each other. This would therefore provide a good chance to pay a special focus to this until now rather neglected stellar system.

Acknowledgements. We would like to thank an anonymous referee for his/her helpful and critical suggestions greatly improving the overall level of the manuscript. This research was supported by the Scientific Research Projects Directorate of Çanakkale Onsekiz Mart University under the Grant No: FHD-2022-4292. This work has made use of data from the European Space Agency (ESA) mission Gaia (*https://www.cosmos.esa.int/gaia*), processed by the Gaia Data Processing and Analysis Consortium (*www.cosmos.esa.int/web/gaia/dpac*). Funding for the DPAC has been provided by national institutions, in particular the institutions participating in the Gaia Multilateral Agreement. We thank the South African Astronomical Observatory (SAAO) for generous observing time. CE and FM thank the South African National Research Foundation and the University of Johannesburg for funding. We do thank the SuperWASP, ZTF, ASAS-SN, KWS, and TESS teams for making all of the observations easily publically available. The research of P.Z. was partly supported by the project Cooperatio – Physics of Charles University in Prague. This research made use of Lightkurve, a Python package for TESS data analysis (Lightkurve Collaboration *et al.* 2018). This publication makes use of data products from the Two Micron All Sky Survey, which is a joint project of the University of Massachusetts and the Infrared Processing and Analysis Center/California Institute of Technology, funded by the National Aeronautics and Space Administration and the National Science Foundation. This research has made use of the SIMBAD and VIZIER databases, operated at CDS, Strasbourg, France and of NASA Astrophysics Data System Bibliographic Services.

REFERENCES

Bahcall J.N., and Soneira R.M. 1980, *ApJS*, **44**, 73.
Bai, Y., Liu, J., Bai, Z., *et al.* 2019, *AJ*, **158**, 93.
Bilir, S., Ak, S., Karaali, S., *et al.* 2008, *MNRAS*, **384**, 1178.
Borkovits, T., Rappaport, S., Hajdu, T., *et al.* 2015, *MNRAS*, **448**, 946.
Chen, K.-Y. 1975, *Acta Astron.*, **25**, 89.
Claret, A., Giménez, A., Baroch, D., *et al.* 2021, *A&A*, **654**, A17.
Crause, L.A., Carter, D., Daniels, A., *et al.* 2016, *Proceedings of SPIE*, **9908**, 990827.
Crause, L.A., Gilbank, D., van Gend, C., *et al.* 2019, *Journal of Astronomical Telescopes, Instruments, and Systems*, **5**, 024007.
Cutri, R.M., Skrutskie, M.F., van Dyk, S., *et al.* 2003, "The IRSA 2MASS All-Sky Point Source Catalog", NASA/IPAC Infrared Science Archive.
Eggenberger, P., Ekström, S., Georgy, C., *et al.* 2021, *A&A*, **652**, A137.
Ekström, S., Georgy, C., Eggenberger, P., *et al.* 2012, *A&A*, **537**, A146.
Gaia Collaboration, Vallenari, A., Brown, A.G.A., *et al.* 2023, *A&A*, **674**, A1.
Gaulme, P., and Guzik, J.A. 2019, *A&A*, **630**, A106.
Giménez, A., and Bastero, M. 1995, *Astrophysics and Space Science*, **226**, 99.
Gray, R.O., and Corbally, C. 2009, "Stellar Spectral Classification". Princeton University Press.
Groote, D., Tuvikene, T., Edelmann, H., *et al.* 2014, Astroplate 2014, Proceedings of a conference held in March 2014 in Prague, Czech Republic. p.53.
ESA 1997, "The Hipparcos and TYCHO Catalogues", *ESA SP Series*, vol. 1200.
Henden, A.A., Levine, S., Terrell, D., *et al.* 2015, AAS Meeting #225, id.336.16.
Houk, N., and Cowley, A.P. 1975, "University of Michigan Catalogue of two-dimensional spectral types for the HD stars", Vol. 1.
Houk, N., and Smith-Moore, M. 1988, "University of Michigan Catalogue of two-dimensional spectral types for the HD Stars", Vol. 4.
Kochanek, C.S., Shappee, B.J., Stanek, K.Z., *et al.* 2017, *PASP*, **129**, 104502.
Lightkurve Collaboration, *et al.* 2018, *Astrophysics Source Code Library*, 1812.013.
Maehara, H. 2014, *Journal of Space Science Informatics Japan*, **3**, 119.
Mas-Hesse, J.M., Giménez, A., Culhane, J.L., *et al.* 2003, *A&A*, **411**, L261.
Mayer, P. 1990, *Bulletin of the Astronomical Institute of Czechoslovakia*, **41**, 231.
McDonald, I., Zijlstra, A.A., and Watson, R.A. 2017, *MNRAS*, **471**, 770.
Mezzetti, M., Predolin, F., Giuricin, G., *et al.* 1980, *A&AS*, **42**, 15.
Mowlavi, N., Eggenberger, P., Meynet, G., *et al.* 2012, *A&A*, **541**, A41.
Ofek, E.O. 2008, *PASP*, **120**, 1128.
Overall, S., and Southworth, J. 2024, arXiv:2401.13397.
Özer, S., and Sürgit, D. 2017, *AIP Conference Proceedings*, **1815**, 080015.
Pecaut, M.J., and Mamajek, E.E. 2013, *ApJS*, **208**, 9.
Perryman, M.A.C., Lindegren, L., Kovalevsky, J., *et al.* 1997, *A&A*, **323**, L49.
Pickles, A., and Depagne, É. 2010, *PASP*, **122**, 1437.
Pojmanski, G. 2002, *Acta Astron.*, **52**, 397.
Popper, D.M. 1983, *AJ*, **88**, 1242.
Popper, D.M. 1998, *PASP*, **110**, 919.
Popper, D.M., and Jeong, Y.-C. 1994, *PASP*, **106**, 189.
Ricker, G.R., Winn, J.N., Vanderspek, R., *et al.* 2015, *Journal of Astronomical Telescopes, Instruments, and Systems*, **1**, 014003.
Schlafly, E.F., and Finkbeiner, D.P. 2011, *ApJ*, **737**, 103.
Schofield, M., Chaplin, W.J., Huber, D., *et al.* 2019, *ApJS*, **241**, 12.
Shappee, B.J., Prieto, J.L., Grupe, D., *et al.* 2014, *ApJ*, **788**, 48.
Southworth, J. 2012, Proceedings of the workshop "Orbital Couples: Pas de Deux in the Solar System and the Milky Way", p.51.

Southworth, J. 2015, *ASP Conf*, **496**, 164.
Spencer Jones, H., and Jackson, J. 1939, "London: Her Majesty's Stationary Office (HMSO)".
Strohmeier, W., Knigge, R., and Ott, H. 1964, *IBVS*, 66.
Strohmeier, W. 1966, *IBVS*, 166.
Strohmeier, W. 1967, *IBVS*, 195.
Tang, S., Grindlay, J., Los, E., *et al.* 2013, *PASP*, **125**, 857.
Tonry, J., and Davis, M. 1979, *AJ*, **84**, 1511.
Torres, G., Andersen, J., and Giménez, A. 2010, *AARv*, **18**, 67.
Wilson, R.E., and Devinney, E.J. 1971, *ApJ*, **166**, 605.
Wright, C.O., Egan, M.P., Kraemer, K.E., *et al.* 2003, *AJ*, **125**, 359.
Zasche, P., Wolf, M., Vraštil, J., *et al.* 2014, *A&A*, **572**, A71.
Zheng, Z., Cao, Z., Deng, H., *et al.* 2023, *ApJS*, **266**, 18.
Zola, S., Rucinski, S.M., Baran, A., *et al.* 2004, *Acta Astron.*, **54**, 299.
Zola, S., Gazeas, K., Kreiner, J.M., *et al.* 2010, *MNRAS*, **408**, 464.